

Fatigue Life Evaluation Method for Foundry Crane Metal Structure Considering Load Dynamic Response and Crack Closure Effect

Qing Dong^{1,*}, Bin He¹ and Gening Xu¹

Abstract: To compensate for the shortcomings of quasi-static law in anti-fatigue analysis of foundry crane metal structures, the fatigue life evaluation method of foundry crane metal structure considering load dynamic response and crack closure effect is proposed. In line with the theory of mechanical vibration, a dynamic model of crane structure during the working cycle is constructed, and dynamic coefficients under diverse actions are analysed. Calculation models of the internal force dynamic change process of dangerous cross-sections and a simulation model of first principal stress-time history are established by using the steel structure design criteria, which is utilised to extract the change of first principal stress of danger points over time. Then, the double-parameter stress spectrum is obtained by the rain flow counting method. The fatigue life calculation formula is corrected by introducing a crack closure parameter that can be calculated by the stress ratio and the effective stress ratio. Under the finite element model imported into Msc. Patran, crack propagation analysis is performed by the growth method in the fatigue integration module Msc. Fatigue. Taking the metal structure of a 100/40t-28.5m foundry crane with track offset as an example, the accuracy of calculation results and the feasibility and applicability of the proposed method are verified by theoretical calculation and finite element simulation, which provide a theoretical basis for improvement of the fatigue resistance design of foundry cranes.

Keywords: Metal structure of foundry crane, load dynamic effect, crack closure effect, crack propagation, fatigue life.

1 Introduction

Foundry cranes are indispensable for achieving automation and intelligence in the modern metallurgical foundry industry, and are special mechanical equipment mainly used to lift, unload, or transport ladle in the modern manufacturing process, which can improve worker efficiency and reduce labour intensity [Kulka, Mantic, Faltinova et al. (2018)].

The typical welded structure of foundry cranes is comparable to general cranes engaged

¹ School of Mechanical Engineering, Taiyuan University of Science and Technology, Taiyuan, China.

* Corresponding Author: Qing Dong. Email: qingdong@outlook.com.

Received: 31 August 2019; Accepted: 19 November 2019.

in a harsh environment with heavy work that includes intermittent, repetitive, cyclic, and frequent start-up and braking. These actions lead to strong impact and vibration of the whole crane structure. Under the cyclic action of impact load, fatigue damage gradually forms in high stress areas of the crane structure, causing metallurgical welding defects. Cracks generated by stress gradually propagate, causing eventual destruction of the structure. Once the structure is destroyed, it will easily lead to overturning of the ladle and the leakage of molten steel, thus threatening the safety of personnel and property [Wei (2019)]. Statistics show that 90% of failure or damage to the mechanical structure and parts is caused by fatigue crack growth [Xiang and Xiao (2015)].

The fatigue life assessment technology of welded structures is one of the assessment conditions for the safe use of cranes in service, and is also the theoretical basis for crane manufacturing design, inspection and repair, and disposal [Wei and Dong (2010)]. At present, experts and scholars worldwide have achieved good results in the prediction and analysis of the fatigue life of welded structures. Among them, Mikkola et al. [Mikkola, Murakami and Marquis (2014)] propose a method for predicting the crack propagation life of welded joints by the equivalent crack length method, and discusses the fatigue life from initial crack propagation to critical cracking under variable amplitude load. The fatigue life prediction model based on elastic fracture mechanics is given in Cui et al. [Cui, Zhang, Bao et al. (2019)], which describes the effects of residual welding stress and residual welding stress relaxation in the fatigue crack propagation of welded joints. For the parts and components of mechanical products, the fatigue residual life estimation is deduced and the reliability is evaluated in a probabilistic manner considering material and process factors on the basis of the field measured data and Bayesian theory, as described in An et al. [An, Choi, Kim et al. (2011)]. Ávila et al. [Ávila, Palma and Paula (2017)] explored safety from the perspective of fatigue life for the rail beam of a foundry crane that has been in service for more than 30 years. The fatigue life analysis of large-scale structural parts is carried out by the nominal stress method modified by the comprehensive fatigue correction coefficient in Huang et al. [Huang (2013); Huang, Huang and Zhan (2012a, b)], which is based on considering the stress concentration factor, component size, and surface state factor. For the fatigue life of the lattice jib structure of cranes in service, Cai et al. [Cai, Wang and Zhao (2013); Cai, Zhao, Gao et al. (2014)] proposes the stress spectrum acquisition method based on K-type welding from the perspective of 'detection, simulation, contrast and statistics', and determines the fatigue life of a welding seam by the nonlinear cumulative damage theory. Taking a quayside crane as the research object, the fatigue life of the trapezoidal frame, tie rod, and the whole crane is analysed by ABAQUS and the Fe-safe combined simulation method [Wu, Duan, Yang et al. (2019)]. Considering the characteristics of crane box girder structure and complex stress conditions, an equivalent crack method based on test data is proposed to estimate fatigue life in Luo et al. [Luo, Wu, Ding et al. (2018)]. Taking the girder of three generations of loop cranes in a nuclear power station as the research object, the finite element model of the girder is established. Finite element analysis is carried out according to the structural particularity of the girder, and the fatigue life is studied based on the crack propagation formula in Chen [Chen (2018)].

The above studies have evaluated the fatigue life of welded structural parts from their respective perspectives, but the results have not reflected the load dynamic effect on the

life and crack closure effect.

Therefore, the metal welding structure of a casting crane is taken as the object of study in this paper. Firstly, the structure dynamics model is established based on mechanical vibration theory, the load impact response is analysed during the working cycle, and the load impact coefficients are obtained under diverse actions. Secondly, the first model using stress-time history theory considering load impact response is established using the design criterion of a steel structure, and the change process over time for the first principal stress is obtained at the danger point. Furthermore, the fatigue life calculation formula is revised by introducing crack closure parameters calculated by the stress ratio and the effective force ratio, forming a fatigue life evaluation model based on fracture mechanics. Finally, taking the metal structure of a 100/40t-28.5m eccentric rail casting crane as an example, the finite element model is imported into Msc. Patran, and crack growth analysis is carried out by the growth method in the fatigue integrated module Msc. Fatigue. Further, the feasibility and applicability of the proposed method are verified by comparing the theoretical results with the results of finite element analysis.

2. Analysis of load shock response during work cycle

One work cycle of a foundry crane denotes an entire sequence of operations, commencing when a load is hoisted and ending at the moment when the appliance is ready to hoist the next load. A work cycle includes the whole crane running, the crab running, and the normal stop, as shown in Fig. 1. The dynamic effect of the hoisting load caused by each action in one work cycle is shown in Fig. 2. The meanings of each symbol are shown in Tab. 1 and Tab. 2.

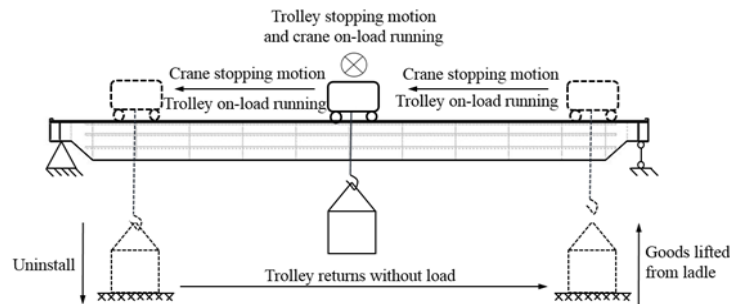


Figure 1: One work cycle of foundry crane

Table 1: Definition of symbols

Symbol	Definition	Symbol	Definition	Symbol	Definition
m_Q	Lifting weight includes lifting gear quality	$0-t_1$	Rising stage	t_4-t_5	Crane running and trolley stopping motion
m_x	Quality of lifting trolley	t_1-t_2	Normal rest	t_5-t_6	Normal rest
m_z	Crane quality	t_2-t_3	Trolley on-load running and crane stopping motion	t_6-t_7	Uninstall
Δm	Quality of removal part	t_3-t_4	Normal rest	t_8-	Start hoisting the next

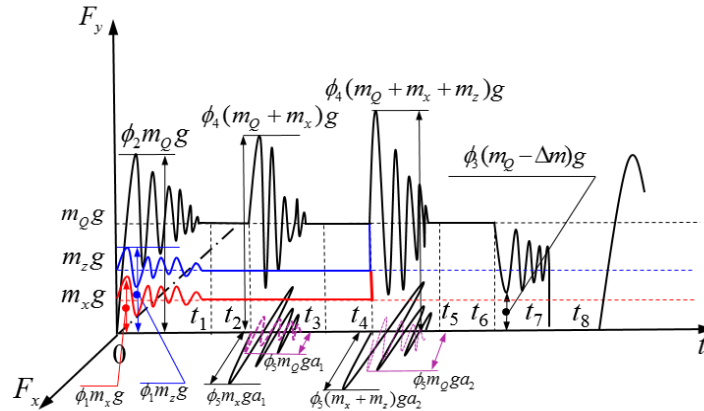


Figure 2: Load dynamic effect under one working cycle

Table 2: Definition of coefficients

Symbol	Definition
Lift impact coefficient ϕ_1	The self-weight of the crane structure itself will increase or decrease impulsively due to the vibration when the weight is lifted off the ground, part of the weight suspended in the air is suddenly removed, or the weight suspended in the air is lowered and braked.
Lifting dynamic load coefficient ϕ_2	When the lifting load is accelerated from the ground, the inertia force of the load increases the static value of the lifting load, which causes elastic vibration of the structure.
Impact coefficient of sudden unloading ϕ_3	During normal operation, part of the lifting mass Δm is suddenly removed from the total lifting mass in the air.
Running impact coefficient ϕ_4	The vertical impact dynamic effect is caused by a crane or trolley moving on uneven track.
Dynamic effect coefficient of structures under catastrophic driving force ϕ_5	Horizontal inertia is caused by a crane or trolley moving along the longitudinal or transverse direction in the horizontal plane.

2.1 Dynamical effect caused by self-weight of structure

The self-weight of the crane structure itself will increase or decrease impulsively due to the vibration when the weight lifts off the ground, part of the weight suspended in the air is suddenly removed, or the weight suspended in the air is lowered and braked. The self-weight vibration load can be defined as $P_G = \phi_1 mg$. ϕ_1 is the lift impact coefficient and the value range of ϕ_1 is from 0.9 to 1.1 [International Standard (2016)]. Compared with the lifting load, the self-weight load contributes less to the fatigue failure of structure. To simplify the calculation, ϕ_1 is equal to a fixed value of 1.1 in the working cycle.

2.2 Dynamic effect caused by rising process

According to the characteristics of foundry crane metal structure and the problems needing to be analysed, the dynamic system in the hoisting process is simplified to a 2-DOF system under the condition of ensuring the accuracy of results, as shown in Fig. 3. In line with the principle of equivalent stiffness, foundry crane metal structure is

simplified to a beam, and the trolley and the main girder are equivalent to one mass block. The lifting gear and ladle are equivalent to the other mass block.

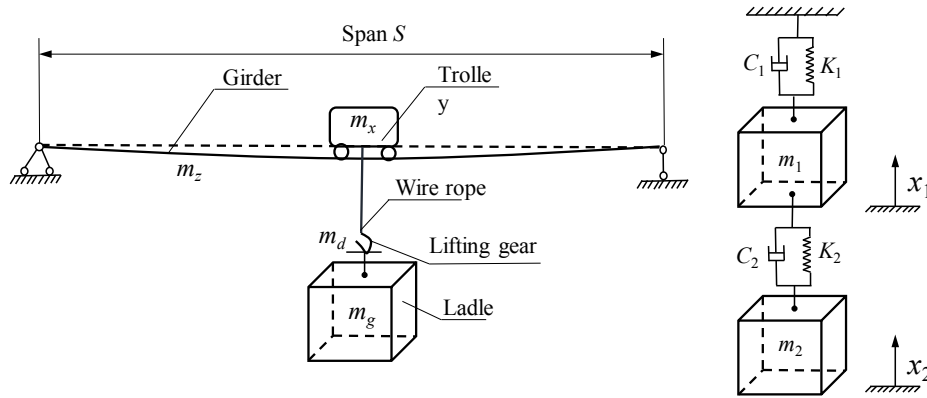


Figure 3: Dynamic model of crane lifting process

There are three stages in the process of lifting the ladle from ground unconstrained. The first stage is when the ladle begins from a static state, the wire rope changes from relaxation to tension, the steel wire rope and beam structure begin to deform, and the load on the lifting gear gradually increases from zero to the weight of ladle. The second stage is when the ladle rises gradually from the ground, and the beam structure displays elastic vibration. The third stage is when the trolley brakes during hoisting. The load changes in each stage are shown in Fig. 4.

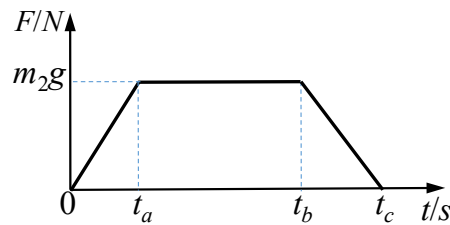


Figure 4: Ramp pulse load

As described in Fig. 2, $0-t_a$ is the first stage of the lifting process, and the linear load can be expressed as $F_1(t) = m_2gt / t_a$. t_a-t_b is the second stage of the lifting process, and the constant load can be defined as $F_2(t) = m_2g$. t_b-t_c is the third stage of the lifting process, and the linear load can be described as $F_3(t) = m_2g(t - t_c) / (t_b - t_c)$.

Based on Fig. 6, the kinetic energy, potential energy, and loss of the crane structure system during hoisting are determined as:

$$\begin{cases} T = \frac{1}{2}m_1\dot{x}_1^2 + \frac{1}{2}m_2\dot{x}_2^2 \\ V = \frac{1}{2}k_1x_1^2 + \frac{1}{2}k_2(x_2 - x_1)^2 \\ R = \frac{1}{2}c_1\dot{x}_1^2 + \frac{1}{2}c_2(\dot{x}_2 - \dot{x}_1)^2 \end{cases} \quad (1)$$

where, T , V , and R are the kinetic energy, potential energy, and loss of the system, respectively. m_1 is the equivalent mass of the trolley and the main girder. m_2 is the equivalent mass of the lifting gear and ladle. k_1 and c_1 are the stiffness and damping coefficients of structures at ladle suspension points. k_2 and c_2 are the rigidity and damping coefficients of the lifting wire rope (Fig. 3).

According to the generalised load (Fig. 4) and system energy formula (1), the Lagrange equation is adopted to derive the motion differential equation of the damped multi-degree-of-freedom system of a crane structure.

$$\begin{bmatrix} m_1 & 0 \\ 0 & m_2 \end{bmatrix} \begin{Bmatrix} \ddot{x}_1 \\ \ddot{x}_2 \end{Bmatrix} + \begin{bmatrix} c_1 + c_2 & -c_2 \\ -c_2 & c_2 \end{bmatrix} \begin{Bmatrix} \dot{x}_1 \\ \dot{x}_2 \end{Bmatrix} + \begin{bmatrix} k_1 + k_2 & -k_2 \\ -k_2 & k_2 \end{bmatrix} \begin{Bmatrix} x_1 \\ x_2 \end{Bmatrix} = \begin{Bmatrix} 0 \\ F_i(t) \end{Bmatrix} \quad (2)$$

where, $F_i(t)$ is the generalised loads, $i=1,2,3$, and t is the time variable. For $i=1$, $F_1(t)$ is the linear load in the first stage of the lifting process, and $0 < t \leq t_a$. For $i=2$, $F_2(t)$ is the constant load in the second stage of the lifting process, and $t_a < t \leq t_b$. For $i=3$, $F_3(t)$ is the linear load in the third stage of the lifting process, as shown in Fig. 4.

The initial conditions for the first stage can be expressed as $t=0$, $x_1 = x_2 = 0$, and $\dot{x}_1 = \dot{x}_2 = 0$. The beginning of the second stage is the end of the first stage, expressed as $t = t_a$, $x_1 = x_1(t_a)$, $x_2 = x_2(t_a)$ and $\dot{x}_1 = \dot{x}_1(t_a)$, $\dot{x}_2 = \dot{x}_2(t_a)$. The beginning of the third stage and the end of the second stage are expressed as $t = t_b$, $x_1 = x_1(t_b)$, $x_2 = x_2(t_b)$, $\dot{x}_1 = \dot{x}_1(t_b)$, and $\dot{x}_2 = \dot{x}_2(t_b)$.

The initial conditions of each stage being given, the fourth-order Runge-Kutta method is used to solve Eq. (2). Thus, the displacement $x_2(t)$ and acceleration response $\ddot{x}_2(t)$ of the centre of mass m_2 can be obtained under the impact load during the lifting process. Furthermore, the dynamic load and lifting dynamic load coefficients of the equivalent mass of the lifting gear and ladle in the lifting process are obtained as follows:

$$\begin{cases} F_{m_2}(t) = m_2\ddot{x}_2(t) \\ \phi_2 = \ddot{x}_2(t) / g \end{cases} \quad (3)$$

where, $F_{m_2}(t)$ is the dynamic load of the equivalent mass of the lifting gear and ladle in

the lifting process; ϕ_2 is the lifting dynamic load coefficient; and g is the gravity acceleration, $g = 9.8 \text{ m} / \text{s}^2$.

2.3 Dynamic effect caused by unloading process

When the grab and electromagnetic sucker of the crane are working normally, it is necessary to be able to suddenly remove part mass Δm_1 from total lifting mass m_1 in the air. The reduced dynamic load lifting is defined as $\phi_3 m_1 g = (1 - \Delta m_1 / m_1 (1 + \beta_3)) m_1 g$, where β_3 is the unloading coefficient, which is greater than 0 and less than $(m_1 - \Delta m_1)g$. According to the above analysis, the contribution of lifting a dynamic load to structural fatigue damage during the unloading process is very small, though it can play an anti-fatigue role in the whole working cycle. Therefore, the dynamic effect of loads during unloading can be neglected. The static lifting load $(m_1 - \Delta m_1)g$ can be used to replace the dynamic lifting load $\phi_3 m_1 g$.

2.4 Dynamic effect caused by crane operation

For differences of construction quality, steel track quality, and installation quality of a factory building foundation, problems such as high-low misalignment or clearance at rail joints inevitably occur in existing foundry cranes. Therefore, the impact effect of load increases during operation, which accelerates the crack propagation process and reduces the service life of welded joints. The specific calculation process of vertical impact coefficient ϕ_4 caused by track defects for a crane is described in Dong et al. [Dong, Xu and Xin (2018)].

2.5 Dynamic effect caused by sudden change of driving force

To reflect the actual elastic effect caused by acceleration or deceleration of a driving mechanism, accidental shutdown of a crane, or sudden failure of a transmission mechanism, The dynamic load factor ϕ_5 of the mechanism drive is multiplied by the change of driving force (or moment) causing a change of speed, and the result is a new addition of force. The increased force acts not only on the parts bearing driving force as dynamic load, but also on the crane and lifting mass as their inertia force. The range of ϕ_5 is from 1.0 to 3.0 [Xu (2018)]. Usually, lower values are applicable to the system where the driving force or braking force changes more smoothly, while higher values are applicable to the system where the driving force or braking force changes more abruptly. The details are shown in Tab. 3.

Table 3: Value range of ϕ_5

Order	Conditions	ϕ_5
1	Calculating rotary centrifugal force	1.0
2	Calculating horizontal inertial force	1.5

3	The transmission system has no clearance and the control system of continuously variable speed is used. The acceleration force or braking force changes continuously and smoothly.	1.2
4	There is a small gap in the transmission system. With other general control systems, the acceleration force changes continuously but unsteadily.	1.5
5	The transmission system has obvious clearance, and the acceleration force changes abruptly and incoherently.	2.0
6	The transmission system has large clearance and the mass spring model cannot be used to estimate accurately.	3.0

3 First stress-time history model considering load impact response

Foundry cranes have the most arduous and harshest working conditions among bridge cranes. Their working characteristics are intermittent, repetitive, cyclic, and include frequent start-up and braking. During use, the metal structure of a foundry crane is subjected to strong impact and vibration. Under the cyclic action of impact load, fatigue damage in high stress areas of the structure gradually forms welding defects, and cracks occur on the structure. These cracks continue to expand until fractures are formed in the structure. Therefore, before evaluating the fatigue life of a foundry crane’s metal structure, it is necessary to determine the danger points of dynamic stress under impact loads.

Based on the operation cycle of foundry cranes (Fig. 5), variation of the bending moment $M_y(t)$ and shear force $F(t)$ at danger points over time are deduced by the structural mechanics theory, as presented in Tab. 4. According to the relative positions of dangerous cross-sections of the main girder and trolley wheel, the first stress-time history theoretical model of danger points is established considering load impact response in the working cycle. The process is shown in Fig. 6, and the specific steps are as follows.

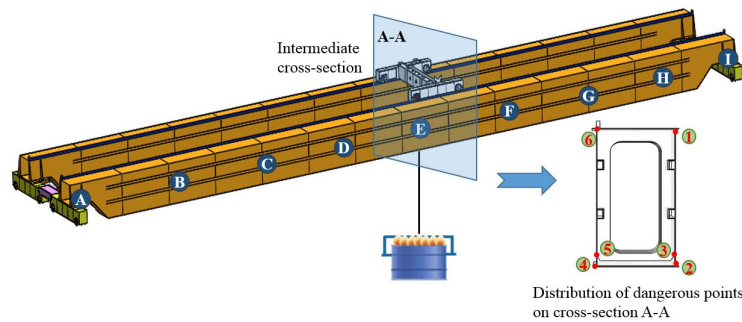


Figure 5: Marked points on main girder and distribution of danger points on a dangerous cross-section

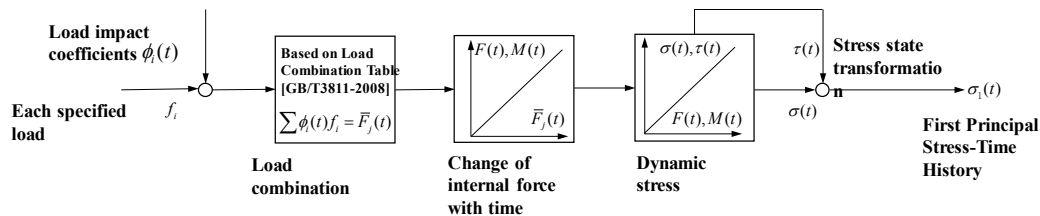


Figure 6: Flow chart of first stress-time history theoretical model considering impact

load response

Fig. 5 shows an illustration of the main girder of a foundry crane with marked trolley position points, as well as danger points on an example cross-section. In operation, the full ladle m_1 is raised at the H point of the right span end, which is the position of the molten iron pit. The lifting trolley with the full ladle then runs to point E of the midspan. After the crane moves to the slag picking position, the trolley runs to the B point of the left span end for slag picking treatment. The trolley with full ladle m_1 then runs to the E point in the middle of the main girder and waits for a few minutes. The crane runs to electric furnace position, and the trolley with the full ladle runs to the of B point, which is the position of the electric furnace at the left span end, and pours molten steel into the furnace, emptying the ladle. While lifting the empty ladle m_2 , the lifting trolley runs to the E point in the middle of the span and the crane runs back to the molten iron pit position. Then, the trolley runs to the H point in the right span, drops the empty ladle, and prepares for the next work action. The frequency of the trolley passing through each marked point on the main girder is given in Tab. 5.

Table 4: Computational models of change process of internal force with time at fatigue danger points in the working cycle

Action	Computational model	Action	Computational model
Rising stage $t \leq t_1$	$\begin{cases} M_y(t) = (\phi_1(t)m_x + \phi_2(t)m_0)g \frac{b(S-L)}{S} + \phi_1(t) \frac{F_q L(S-L)}{2} \\ F(t) = \frac{(\phi_1(t)m_x + \phi_2(t)m_0)gb}{S} + \phi_1(t)F_q(L - \frac{S}{2}) \end{cases}$	Normal rest $t_1 \leq t \leq t_2$	$\begin{cases} M_y(t) = (m_x + m_0)g \frac{b(S-L)}{S} + \frac{F_q L(S-L)}{2} \\ F(t) = \frac{(m_x + m_0)gb}{S} + F_q(L - \frac{S}{2}) \end{cases}$
Trolley load running and crane stopping motion $t_2 \leq t \leq t_3$	$\begin{cases} M_y(t) = \phi_1(t)(m_x + m_0)g \frac{(S-L)v_x(t-t_2)}{S} + \phi_1(t) \frac{F_q L(S-L)}{2} \\ F(t) = \frac{\phi_2(t)(m_x + m_0)gv_x(t-t_2)}{S} + \phi_1(t)F_q(L - \frac{S}{2}) \end{cases}$	Normal rest $t_3 \leq t \leq t_4$	$\begin{cases} M_y(t) = (m_x + m_0)g \frac{(S-L)v_x t_2}{S} + \frac{F_q L(S-L)}{2} \\ F(t) = \frac{(m_x + m_0)gv_x t_2}{S} + F_q(L - \frac{S}{2}) \end{cases}$
Crane running and trolley stopping motion $t_4 \leq t \leq t_5$	$\begin{cases} M_y(t) = \phi_1(t)(m_x + m_0)g \frac{(S-L)v_x t_2}{S} + \phi_1(t) \frac{F_q L(S-L)}{2} \\ M_x(t) = \phi_2(t)(m_x + m_0)ga \frac{(S-L)v_x t_2}{S} + \phi_2(t) \frac{F_q aL(S-L)}{2} \\ F(t) = \phi_2(t) \frac{(m_x + m_0)gav_x t_2}{S} + \phi_2(t)F_q a(L - \frac{S}{2}) \end{cases}$	Normal rest $t_5 \leq t \leq t_6$	$\begin{cases} M_y(t) = (m_x + m_0)g \frac{(S-L)v_x t_2}{S} + \frac{F_q L(S-L)}{2} \\ M_x(t) = (m_x + m_0)ga \frac{(S-L)v_x t_2}{S} + \frac{F_q aL(S-L)}{2} \\ F(t) = \frac{(m_x + m_0)gav_x t_2}{S} + F_q a(L - \frac{S}{2}) \end{cases}$
Uninstall $t_6 \leq t \leq t_7$	$\begin{cases} M_y(t) = m_x g \frac{(S-L)v_x t_2}{S} + \frac{F_q L(S-L)}{2} \\ F(t) = \frac{m_x gv_x t_2}{S} + F_q a(L - \frac{S}{2}) \end{cases}$	No-load Operation of crane $t_7 \leq t \leq t_8$	$\begin{cases} M_y(t) = \phi_1(t)m_x g \frac{(S-L)v_x t_2}{S} + \phi_1(t) \frac{F_q L(S-L)}{2} \\ M_x(t) = \phi_2(t)m_x ga \frac{(S-L)v_x t_2}{S} + \phi_2(t) \frac{F_q aL(S-L)}{2} \\ F(t) = \phi_2(t) \frac{m_x gav_x t_2}{S} + \phi_2(t)F_q a(L - \frac{S}{2}) \end{cases}$
No-load running process of Trolley $t_8 \leq t \leq t_9$	$\begin{cases} M_y(t) = \phi_1(t)(m_x + m_0)g \frac{(S-L)(L-v_x(t-t_8))}{S} + \phi_1(t) \frac{F_q L(S-L)}{2} \\ F(t) = \frac{\phi_2(t)(m_x + m_0)g(L-v_x(t-t_8))}{S} + \phi_1(t)F_q(L - \frac{S}{2}) \end{cases}$	Note: V_x is the running speed of the trolley; V_d is the running speed of the crane; S is the span of main girder; t is time; L is the distance of main girder support point to a dangerous cross-section.	

Table 5: Frequency of trolley passing through marked points on main girder

Marked points	B	C	D	E	F	G	H
Frequency under full ladle lifting	2	3	3	2	1	1	1
Frequency under empty ladle lifting	1	1	1	1	1	1	1

In line with ‘GB/T 3811-2008 Crane Design Code’ [National Standards of the People’s Republic of China (2008)], the normal stress of fatigue danger points of the metal structure of a foundry crane is defined as:

$$\sigma(t) = 1.15 \left(\frac{M_x(t)}{W_x} + \frac{M_y(t)}{W_y} \right) \quad (4)$$

where, $\sigma(t)$ is the normal stress of the fatigue danger point, tensile stress is positive, and compressive stress is negative. $M_x(t)$ and $M_y(t)$ are the bending moments of the dangerous section for x and y axes. W_x and W_y are the section moduli for x and y axes. ‘1.15’ is the coefficient of free bending, restrained bending, and restrained torsion of the box section of the main girder [Xu (2018)].

The shear stress of a fatigue danger point on the web of metal structure of a foundry crane can be expressed as:

$$\tau(t) = \frac{F(t)S_x}{I_x\delta} \quad (5)$$

where, $\tau(t)$ is the shear stress of a fatigue danger point, $F(t)$ is the shear force of a dangerous cross-section, S_x is the static moment of a dangerous cross-section, I_x is the inertia moment of dangerous cross-section, and δ is the web thickness.

Brown and Miller put forward the multiaxial fatigue critical surface theory [Brown and Miller (1973)]. They point out that two strain parameters, cyclic shear strain and normal strain, need to be described in the fatigue process. Concerning the metal structure of casting crane, fatigue cracks usually occur at the position of the maximum three-dimensional stress under complex multi-axis stress conditions. The crack initiation plane is the plane with the largest shear stress amplitude, and the crack propagation direction is the vertical direction of the maximum tensile stress (i.e., the first principal stress). Therefore, it is necessary to transform the normal stress and shear stress of a fatigue danger point into the first principal stress by using the multiaxial fatigue critical surface theory.

The first principal stress of a fatigue danger point is defined as Eq. (6) by the binomial stress state transformation formula:

$$\sigma_1(t) = \frac{\sigma(t)}{2} + \sqrt{\left(\frac{\sigma(t)}{2}\right)^2 + \tau(t)^2} \quad (6)$$

where, $\sigma_1(t)$ is the first principal stress of fatigue dangerous point.

4 Fatigue life assessment model based on fracture mechanics

4.1 Eliminating effect of stress ratio

Before evaluating the fatigue residual life of metal structures of foundry cranes, it is necessary to extract the two-dimensional stress spectrum, including stress mean spectrum and stress amplitude spectrum. to eliminate the influence of average stress, according to the principle of equal life, Goodman formula $\sigma_{Ra} / \sigma_{-1} + \sigma_{Rm} / \sigma_b = 1$ is used to transform all amplitude stress into stress variation $\Delta\sigma$ under cyclic characteristic $R=0$ [Tao (2012)].

$$\Delta\sigma = \frac{2(\sigma_{Ra} + \frac{\sigma_{-1}}{\sigma_b} \sigma_{Rm})}{1 + \frac{\sigma_{-1}}{\sigma_b}} \quad (7)$$

where, σ_{-1} is the fatigue strength of materials for $R=-1$. σ_b is the ultimate strength of materials, being either the ultimate tensile strength of high-strength brittle materials or the yield strength of ductile materials [Chen (2002)]. σ_{Rm} is the mean stress for cyclic characteristic R , σ_{Ra} is the stress amplitude for cyclic characteristic R , and $\Delta\sigma$ is the stress range for cyclic characteristic $R=0$.

4.2 Root mean square equivalent stress method

During the whole operation cycle, the foundry crane bears two kinds of lifting loads, i.e., full ladle lifting and empty ladle lifting. The two-parameter stress spectrum extracted from the first principal stress-time history of each danger point is a variable amplitude spectrum considering the dynamic effect of loads. Therefore, the equivalent stress method should be utilised to transform the variable amplitude stress spectrum into the equal amplitude stress spectrum. The transformation formula is given as:

$$\bar{\sigma} = \left(\frac{\sum \sigma_i^\alpha n_i}{\sum n_i} \right)^{1/\alpha} \quad (9)$$

where, $\bar{\sigma}$ is the equivalent stress amplitude, in MPa; σ_i is the stress amplitude of grade i ($i=1,2,\dots,8$); n_i is the cycles corresponding to the stress amplitude of grade i ; and α is the damage equivalent parameter. For $\alpha=2$, Eq. (9) is the root mean square model.

4.3 Fatigue life assessment considering crack closure effect

In engineering, there are two common methods for estimating the influence of residual stress on fatigue crack growth. One is to treat it as a simple superposition of mechanical parameters playing the same role as the external load. The other is to unify the crack growth behaviour with or without residual stress from the angle of crack closure.

Elber first proposed the concept of plastic-induced crack closure. He believed that when the overload peak was applied, the crack tip would produce larger residual tensile strain, as the negative opening displacement would occur at the crack tip. With the residual tensile strain being formed at the crack tip, crack closure will occur prematurely at the crack tip during unloading. The proposed closure effect of plastic cracks provides a new understanding of fatigue crack growth, and the factors controlling crack growth rate are no longer the range of intensity factor ΔK , but are instead the effective stress intensity factor ΔK_{eff} . At present, the research on crack closure is mainly focused on the characterisation of crack closure by crack closure coefficient U [Han, Yang and Dong (2017)].

For fatigue crack growth life analysis under constant amplitude stress, the crack growth life of foundry cranes can be calculated by integrating the crack growth formula considering crack closure effect $da/dN = C_p (U\Delta K)^m$. Meanwhile, in combination with the number of working cycles per year n_y , the crack propagation life of foundry cranes can be obtained using Eq. (10) for the stress ratio $R=0$.

$$N_y = \frac{1}{n_y} \begin{cases} \frac{1}{C_p (UY\bar{\sigma}\sqrt{\pi})^m (0.5m-1)} \left(\frac{1}{a_0^{0.5m-1}} - \frac{1}{a_c^{0.5m-1}} \right) & (m \neq 2) \\ \frac{1}{C_p (UY\bar{\sigma}\sqrt{\pi})^m} \ln \left(\frac{a_c}{a_0} \right) & (m = 2) \end{cases} \quad (10)$$

where, a_0 is the initial crack size, in mm; a_c is the critical crack size, in mm; Y is the geometric correction factor; C_p and m are material parameters; n_y is the number of working cycles per year for foundry crane, in cycles; N_y is the crack propagation life of foundry cranes, in years; and U is the crack closure effect parameter, defined as Eq. (11) in Khaburskiy et al. [Khaburskiy, Slobodyan, Hredil et al. (2019)].

$$\begin{cases} U = \frac{1-q}{1-R} \\ q = 0.31 \left(1 + \frac{R}{0.74} \right) \end{cases} \quad (11)$$

For $m \neq 2$, the relationship between fatigue crack growth size a_i and fatigue residual life N_i of foundry cranes can be obtained as:

$$a_i = \left[\left(\frac{1}{a_0} \right)^{0.5m-1} - N_i (0.5m-1) n_y C_p (UY\bar{\sigma}\sqrt{\pi})^m \right]^{\frac{2}{2-m}} \quad (12)$$

where, a_i is the fatigue crack growth size, $a_0 \leq a_i \leq a_c$; and N_i is the fatigue life of crane

extending from a_0 to a_i .

4.4 Parameters determination

1) Initial crack and critical crack

Fracture mechanics assumes that a structural member has an initial crack, so the initiation stage of the crack can be neglected, but the size of the initial crack does not have a standard value. Therefore, it is necessary to determine the initial crack length a_0 by fracture mechanics when calculating the crack growth life of the metal structure of a foundry crane. According to existing non-destructive crack detection technology, the initial crack size can be considered in the range of 0.5-2 mm. For a conservative assumption, the value is 0.5 mm. The crack propagates gradually until fatigue fracture after enough cycles under varying loads. At this point, the critical value of the crack a_c can be expressed as:

$$a_c = \frac{K_{IC}^2}{\pi Y^2 \sigma^2} \quad (13)$$

The critical crack size a_c is related to the material. From relevant literatures and historical test data [Zhai and Wang (1994, 1996)], the critical crack growth rate of metal structure of foundry crane under the stress cycle can be obtained as $v_c = 2.54 \times 10^{-3}$ mm/cycle. On the basis of the formula ‘ $da/dN = C_p (\Delta K)^m$ ’, the relationship between crack growth rate and fracture toughness can be described as Eq. (14):

$$v_c = CK_{IC}^m \quad (14)$$

The relationship between critical crack size a_c and critical crack growth rate v_c can be obtained by transforming Eq. (10) and substituting it to Eq. (9).

$$a_c = \frac{v_c^{2/m}}{\pi C^{2/m} Y^2 \sigma^2} \quad (15)$$

where, a_c is the critical crack size; and v_c is the critical crack growth rate.

2) Crack growth threshold and fracture toughness

In the first stage of crack growth, there exists a lower limit value of the stress intensity factor, which means that crack growth does not occur under external variable loads and the lower limit value is the crack growth threshold ΔK_{th} . Because the crack growth threshold is easily affected by the cyclic stress ratio $R = K_{min}/K_{max}$, the empirical formula for the crack growth threshold is determined by the mathematical statistics and fitting of experimental data based on the fixed value of cyclic stress ratio R.

The empirical formula is given by Barsom based on the experimental data in Zhan [Zhan (2014)].

$$\Delta K_{th} = \begin{cases} 6.4(1-0.85R), & R > 0.1 \\ 5.5, & R \leq 0.1 \end{cases} \quad (16)$$

where, R is the cyclic stress ratio, $R = \frac{K_{\min}}{K_{\max}}$. K_{\min} and K_{\max} are the stress intensity factors for the minimum and maximum stress in $\text{MPa}\sqrt{\text{m}}$. ΔK_{th} is the crack growth threshold in $\text{MPa}\sqrt{\text{m}}$.

The amplitude of stress intensity factor ΔK increases with stress amplitude $\Delta\sigma$. When the stress amplitude increases to a certain value, the stress intensity factor amplitude just crosses the threshold value of stress intensity factor, namely $\Delta K > \Delta K_{th}$. The crack in the metal structure begins to expand under the external variable load and until the amplitude of the stress intensity factor reaches a certain value at which failure occurs, causing a fracture of the metal structure. The certain value is defined as fracture toughness K_{IC} .

The fracture toughness of material K_{IC} is the test value. In line with the national standard GB4161-84, the stress intensity factor of three-point bending specimen [Chen (2002)] is given as:

$$K_{IC} = \frac{3PL}{2BW^2} \sqrt{\pi a} \left[1.090 - 1.735 \left(\frac{a}{W} \right) + 8.20 \left(\frac{a}{W} \right)^2 - 14.18 \left(\frac{a}{W} \right)^3 + 14.57 \left(\frac{a}{W} \right)^4 \right] \quad (17)$$

The stress intensity factor of standard compact tensile specimens [Chen (2002)] is described as:

$$K_{IC} = \frac{P\sqrt{a}}{BW} \left[29.6 - 185.5 \left(\frac{a}{W} \right) + 655.7 \left(\frac{a}{W} \right)^2 - 1017.0 \left(\frac{a}{W} \right)^3 + 638.9 \left(\frac{a}{W} \right)^4 \right] \quad (18)$$

3) Determining material parameters CP, m, and geometric correction coefficient Y

The fatigue crack growth rate parameters CP and m are measured by fatigue fracture testing, but the material parameters are related to the material, ambient temperature, crack type, and structure shape. For the metal structure material of a foundry crane, the crack growth characteristic parameters of Q345 steel are determined by a standard three-point bending specimen test according to the national fatigue fracture test standard, namely $C_p = 1.06 \times 10^{-13}$, $m = 4.66$.

There are three common kinds of cracks in construction machinery: central cracks, edge cracks, and surface cracks, as shown in Fig. 7.

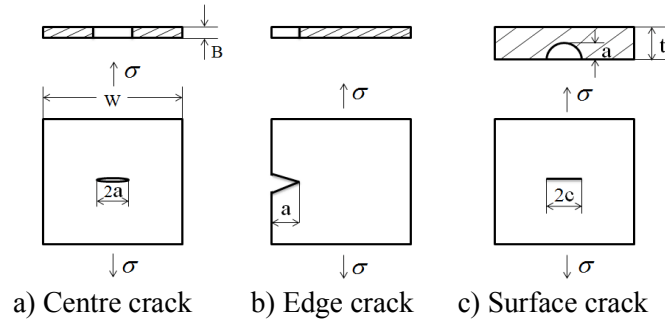


Figure 7: Common cracks

As shown in Fig. 7, central cracks and edge cracks are penetrating cracks, and their sizes can be expressed by mathematical length. Centre cracks propagate along the direction of crack length, which can be expressed as $2a$. For an edge crack, the crack length can be regarded as half of the whole central crack, and can be defined as a . The shape of a surface crack is semi-elliptical, and generally occurs on the surface of structure without penetrating the thickness of structure. The size of a surface crack can be expressed by two parameters, using the crack length $2c$, and the crack propagation depth a .

In the process of fatigue crack propagation analysis in metal structures, the crack shape has an effect on the calculation of crack propagation. For the central penetrating crack, the influence coefficient on crack growth analysis [Zhan (2014)] is as follows:

$$Y = \sqrt{\sec\left(\frac{\pi a}{2W}\right)} \tag{19}$$

where, a is half the length of the crack; and W is the plate width.

For surface cracks, the influence factors on crack growth analysis [Zhan (2014)] are defined as:

$$Y = \frac{\sqrt{\left(\sin^2 \theta + \left(\frac{a}{c}\right)^2 \cos^2 \theta\right)}}{E(k)} M_f \tag{20}$$

where, c is half the length of an elliptical crack.

where, C is half the length of a semi-elliptical crack; θ is the included angle; $E(k)$ is the second kind of complete elliptic integrals; and M_f is the influence coefficient of plate width and thickness.

$$M_f = M_1 + M_2 \left(\frac{a}{t}\right)^2 + M_3 \left(\frac{a}{t}\right)^4 g f_w \tag{21}$$

$$\begin{cases} M_1 = 1.13 - 0.09a/c \\ M_2 = -0.54 + 0.89/(0.2 + a/c) \\ M_3 = 0.5 - 1/(0.6 + a/c) + 14(1 - a/c)^{24} \\ g = 1 + \left[0.1 + 0.35(a/t)^2 \right] (1 - \sin \theta)^2 \\ f_w = \sec(\pi c / 2W \sqrt{a/t})^{0.5} \end{cases} \quad (22)$$

where, t is the plate thickness, and f_w is the shape coefficient of stress intensity factor for penetrating cracks.

5 Engineering examples

Taking a 100/40t-28.5m foundry crane with orbital offset as an example, the whole structure of the crane is shown in Fig. 5. The material of the whole structure is Q345 steel, the working level is A6, and parameters of the foundry crane are given in Tab. 6 and Tab. 7. The number of full ladle lifting actions is 60 times per day ($N_{Q1}=60$ times) and the number empty ladle lifting actions is 60 times per day ($N_{Q2}=60$ times). The number of working days is 365 per year, namely $t_d=365$ days.

Table 6: Parameters of foundry crane

Definition	Values	Unit	Definition	Values	Unit
Span	28500	mm	Distance from the top of the trolley track to the lower edge of the upper cover plate	221	mm
Base distance of crane	6700	mm	Wheel pressure at full load	500000	N
Wheelbase of hoisting trolley	5000	mm	Wheel pressure at no load	220000	N
Track gauge of hoisting trolley	6200	mm	Sum of wheel pressures of main driving wheels at full load	2200000	N
Speed of crane	60	m/min	Sum of wheel pressures of main driving wheels at no load	1040000	N
Hoisting speed	7	m/min	Sum of maximum wheel pressure of crane under lateral force	1100000	N
Limit distance	300	mm	Uniform load caused by self-weight of main girder	20	N/mm

Table 7: Parameters of main girder and end girder of foundry crane with orbital offset

Parameters	Values (mm)	Parameters	Values (mm)
Main web thickness of main girder (Central section)	10	Gap between webs of main girder	1900
Accessory web thickness of main girder (Central section)	8	Gap between cover plates of main girder	2400
Main web thickness of main girder (End section))	18	Head web height of main girder	991
Accessory web thickness of main girder (End section)	16	Diaphragm thickness	10
Thickness of lower cover plate of main girder (Central section)	12	Thickness of cover plate of end girder	10
Thickness of lower cover plate of main girder (End	20	Web thickness of end girder	8

section)			
Thickness of upper cover plate of main girder	12	Spacing between end beam webs	604
Width of upper cover plate of main girder	2155	Spacing between end beam cover plates	991
Width of lower cover plate of main girder	2000	Thickness of end girder diaphragm	10

5.1 First stress-time history considering dynamic effect of load

According to the analysis process of load impact response during the working cycle, the first stress-time history theory model considering the load dynamic effect is used to simulate and analyse the metal structure of a foundry crane with orbital offset. The change process over time is extracted for the first principal stress at the danger point. The simulation result for danger point 2 is given in Fig. 8. The analysis results for the remaining danger points are similar to that of point 2 and will not be further elaborated.

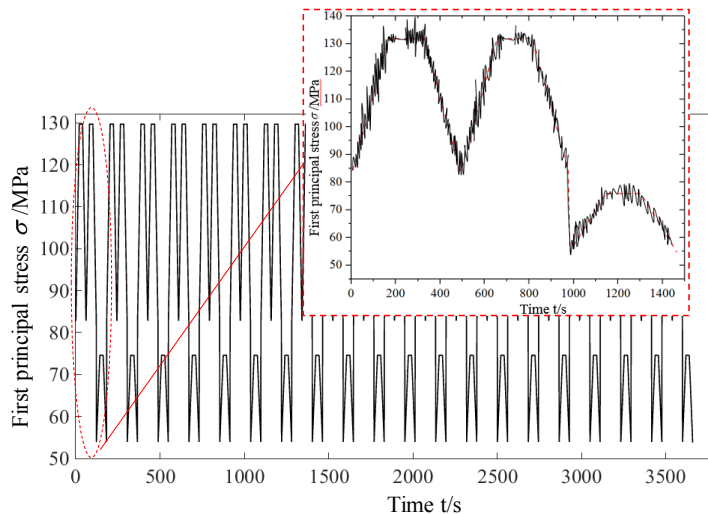
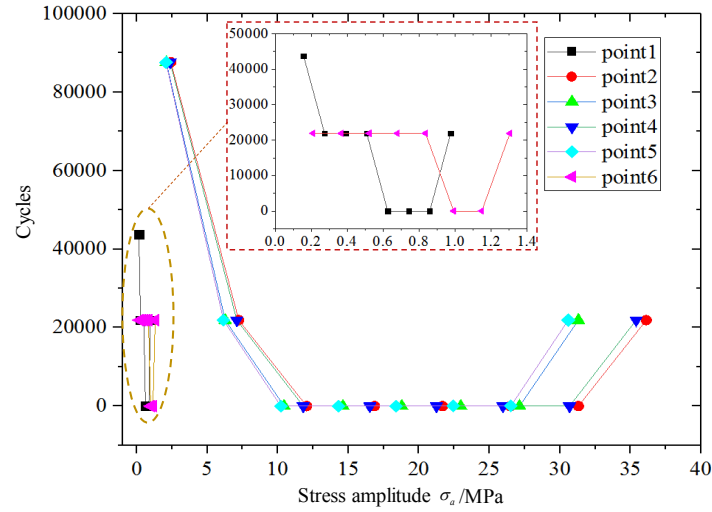


Figure 8: First principal stress-time history simulation for danger point 2

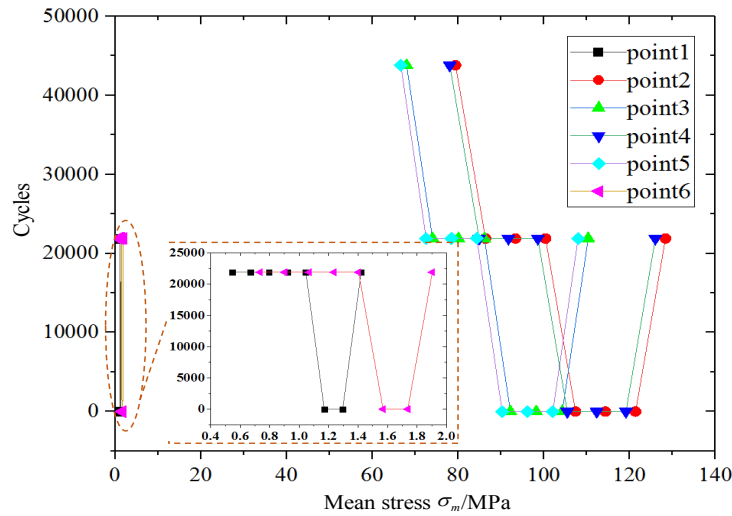
Fig. 8 shows the simulation results of the first principal stress-time history in 20 working cycles. The dynamic load effect is disturbed along the straight line segment (oblique straight line) with no dynamic load effect in each working cycle. The maximum effect discrepancy can be up to 9.85 MPa, which occurs in the running stage of the crane bearing loads under each action.

5.2 Fatigue life

The rain flow counting method is used to extract the two-parameter stress spectrum from the simulation results of the first principal stress-time history of each danger point. The results are described in Fig. 9.



a) stress amplitude spectrum



b) stress mean spectrum

Figure 9: Two-parameter stress spectrum of dangerous points

Fig. 9 describes the eight-level two-parameter stress spectrum of each danger point. Compared with the danger points from point 2 to point 5, the stress amplitude and stress mean values of point 1 and point 6 are smaller at all levels. The reason is that point 1 and point 6 are in the compressive stress region, and the calculation results of the first principal stress are smaller after the transformation of the binomial stress state. According to the parameter determination method in Section 4.4, fracture performance parameters of the metal structure material Q345 of foundry crane were obtained, and are shown in Tab. 8.

Table 8: Fracture performance parameters of material

Fracture properties of material	Values
Ultimate strength	470 MPa
Modulus	2.1E5 MPa
Fatigue strength without notch	167.8 MPa
Fracture toughness K_c	77.25 MPa \sqrt{m}
Coefficient C_P	1.06E-13
Index m	4.66
Y	1.18
Threshold of stress intensity factor of ideal crack tip $\Delta K (R=0)$	5.38 MPa \sqrt{m}
Threshold of stress intensity factor of non-ideal crack tip ($R \rightarrow 1$)	2 MPa \sqrt{m}

Based on the above, the initial crack length is 0.5 mm, and the equivalent stress, critical crack size, and crack propagation life at each danger point are calculated by using the sum of Eqs. (8)-(11) and Eq. (13). The results are shown in Tab. 9.

As given in Tab. 9, the maximum equivalent stress of danger point 2 is 92.52MPa, the minimum critical crack size is 124.4 mm, and the shortest crack growth life is 37.37 years. Therefore, the danger point 2 is taken as an example to analyse the crack growth process. The results are shown in Tab. 10 and Fig. 10.

Table 9: Crack propagation life at danger points

Derived value	Point 1	Point 2	Point 3	Point 4	Point 5	Point 6
Equivalent stress (MPa)	1.3563	92.52	80.53	92.17	74.32	1.0211
Critical crack size (mm)	4.11E+5	124.4	150.8	128.4	159.2	2.01E+5
Crack propagation life (years)	7.13E+9	37.37	74.64	39.28	84.19	1.75E+9

Table 10: Fatigue life corresponding to crack propagation size of point 2

Crack growth size (mm)	Fatigue life (years)	Crack growth size (mm)	Fatigue life (years)	Crack growth size (mm)	Fatigue life (years)
0.5	0	5.0	35.64	50.0	37.31
0.6	8.05	6.0	36.02	60.0	37.32
0.7	13.49	7.0	36.28	70.0	37.34
0.8	17.38	8.0	36.46	80.0	37.34
0.9	20.28	9.0	36.59	90.0	37.35
1.0	22.52	10.0	36.70	100.0	37.36
2.0	31.48	20.0	37.12	110.0	37.36
3.0	33.94	30.0	37.23	120.0	37.36
4.0	35.04	40.0	37.28	124.4	37.37

From Tab. 10 and Fig. 10, it can be seen that the fatigue life is 8.05 years when the crack extends from 0.5 mm to 0.6 mm as time progresses. By analogy, it takes 37.37 years for the crack to extends the critical crack. Before 20.28 years, the crack growth rate is relatively slow. From 20.28 years to 35.04 years, the crack growth rate is relatively fast. After 35.04 years, the crack propagation speed is very fast. By 37.37 years, the crack reaches the critical value and a fatigue fracture will occur.

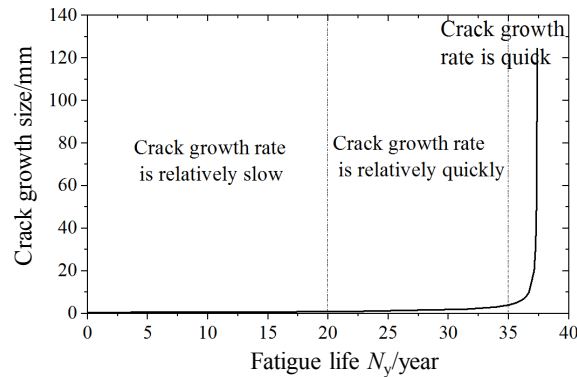


Figure 10: Crack Propagation Process of danger point 2

5.3 Finite element analysis of fatigue crack propagation based on Msc. Fatigue

In line with the parameters of a 100/40t-28.5m foundry crane with orbital offset (see Tab. 6) and the parameters of the main girder (Tab. 7), the APDL language of finite element software ANSYS is used to model the main girder. The model is imported into Msc. Patran in IGS format. The growth method in the fatigue integration module Msc. Fatigue ([Liu (2012)]) is utilised to analyse the crack growth.

1) Failure criterion

According to the formula of stress intensity factor $K=Y\sigma\sqrt{\pi a}$, the stress amplitude and crack growth size are proportional to the stress intensity factor. The fatigue crack growth rate da/dN can also be expressed by the amplitude of stress intensity factor ΔK from the $da/dN - \Delta K$ curve. As shown in Fig. 11, the fatigue crack growth rate can be divided into three regions: low, medium, and high.

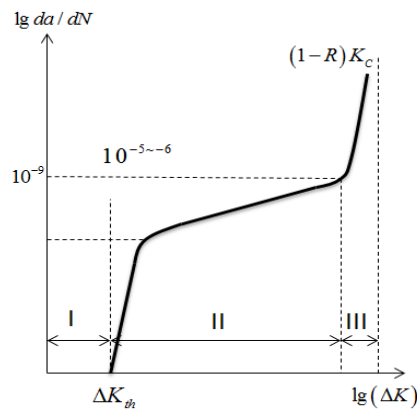


Figure 11: $da/dN - \Delta K$ curve

Region I: Low expansion rate stage. In this stage, the crack growth rate decreases greatly with decreased stress intensity factor amplitude, and for $\Delta K \leq \Delta K_{th}$, it can be considered

that fatigue crack growth did not occur. Region II: Medium crack growth rate stage. The research shows that the function relation in this stage is the famous Paris formula, and the $da/dN - \Delta K$ curve has a good logarithmic linear relationship. The evaluation of fatigue crack growth life based on this relationship is the focus of the fatigue fracture research. Region III: High crack growth rate stage. In this stage, the fatigue crack growth rate increases rapidly, and fatigue life is so short that it can be neglected.

Hence, regarding region II as the research object, and in line with the linear elastic fracture criterion, the failure criterion of component [Wang (2009)] is given as follows:

$$K_{\max} = Y\sigma_{\max}\sqrt{\pi a} \geq K_{IC} \text{ or } a \geq a_c \tag{23}$$

where, σ_{\max} is the maximum cyclic stress, a is the crack size, a_c is the critical crack size.

2) Set of loads and material properties

The analysis of fatigue crack growth mainly studies the medium rate stage in crack propagation. In the process of fatigue crack growth analysis, it is necessary to set material information according to material fracture parameters and create relevant material information plates in software. The fracture performance parameters of foundry crane material are described in Tab. 8.

The material relationship curve $da/dN - \Delta K$ is obtained based on the ratio of maximum stress to minimum stress $R=0.4$ in the first principal stress-time history of danger point 2, as shown in Fig. 13. In addition, a group of nodes should be created to represent the far-field stress. The stress of nodes in the creation group is averaged to calculate the stress intensity factor.

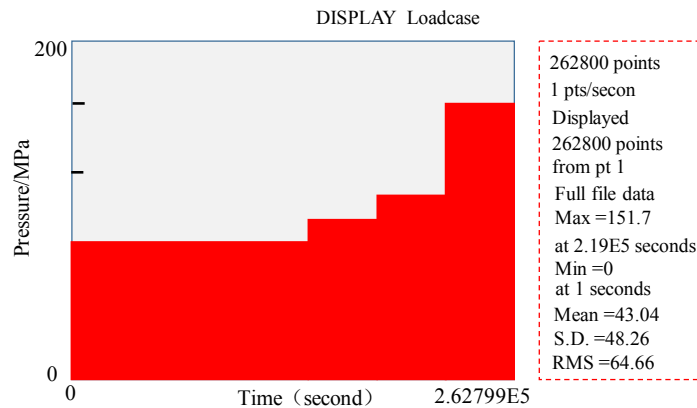


Figure 12: Midspan load setting

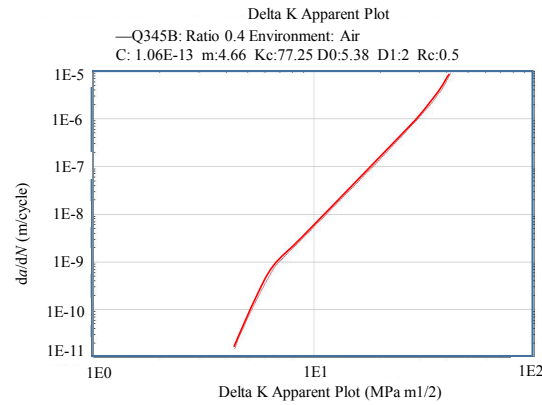


Figure 13: Curve of $da / dN - \Delta K$ for material

3) Flexible function generation

The standard sample model of crack growth should be established before the analysis of fatigue crack growth. The actual crack shape of the welded box girder structure of a foundry crane is equivalent to the unilateral crack tension specimen by using Msc. Fatigue. The relevant parameters are set. In Fig. 14(a), the thickness of specimen B is 10mm, and width W is 2000 mm. Fig. 14(b) shows the corresponding flexible function curve obtained by the operation.

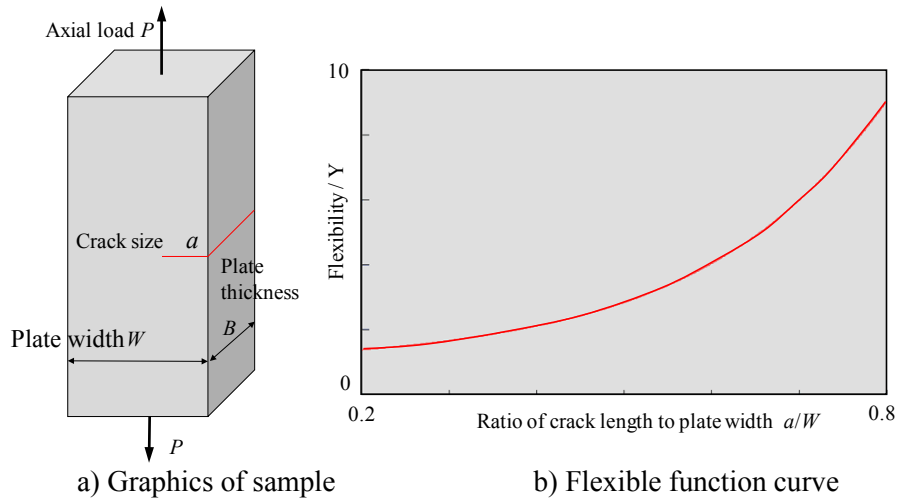


Figure 14: Graphics of sample and flexible function curve

4) Analysis results of fatigue crack growth

The fatigue crack growth is analysed by using Msc. Fatigue. The results are shown in Tab. 11.

Table 11: Analysis results of crack growth

Fatigue life (years)	Number of cycles	Failure form	Critical crack size (mm)	Crack growth rate (m/cycle)	Apparent stress intensity factor amplitude (MPa√m)	Effective stress intensity factor amplitude / MPa√m	Crack closure (MPa√m)	Static fracture (MPa√m)	Effective stress ratio
37.69	4952438	A*	128.1	4.776E-5	68.95	71.95	5.292	8.312	0.06851

A*-the amplitude of effective stress intensity factor exceeds the fracture toughness or the amplitude of critical stress intensity factor

Failure of the welded box girder structure of a foundry crane occurs when the amplitude of effective stress intensity factor exceeds the fracture toughness or the amplitude of critical stress intensity factor. From Tab. 11, the crack growth size reaches 128.1 mm, the number of working cycles is 4,952,438 (37.69 years), and the crack growth rate is 4.776E-5 m/cycle when fatigue failure occurs.

In Tab. 11, there are two kinds of stress intensity factor amplitudes, including apparent stress intensity factor amplitude ΔK_{app} and effective stress intensity factor amplitude ΔK_{eff} . The crack propagation occurs only when the crack opens. It is not the stress intensity factor amplitude ΔK , but the effective stress intensity factor amplitude ΔK_{eff} that causes the crack propagation, which can be expressed as:

$$\Delta K_{eff} = \begin{cases} K_{max} - K_{min} & \text{unclosed} \\ K_{max} - K_{op} & \text{closed} \end{cases} \quad (24)$$

The relationship between crack growth rate and the stress intensity factor amplitude of the welded box girder structure of a foundry crane is shown in Fig. 15. The relationship between fatigue crack growth size and the number of cycles (fatigue life) is shown in Fig. 16.

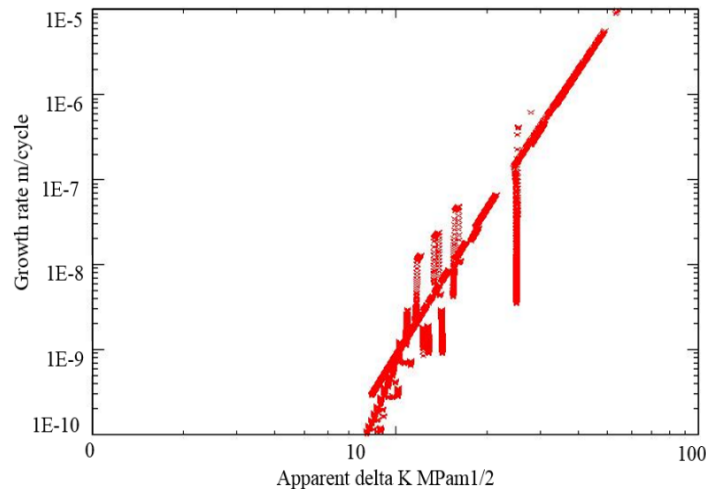


Figure 15: $da / dN - \Delta K$ curve

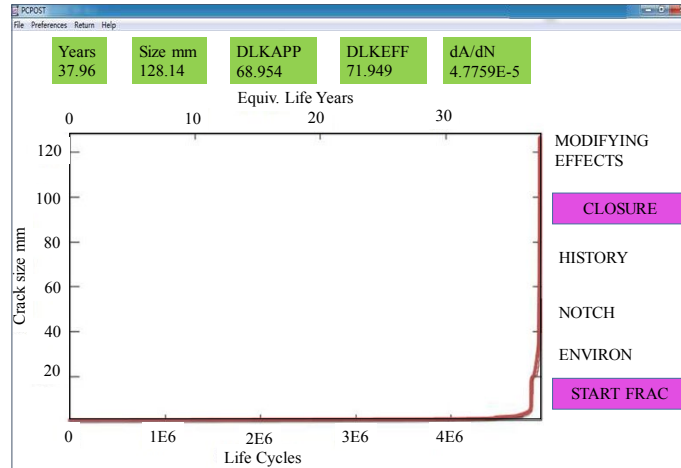


Figure 16: Fatigue life curve corresponding to crack size

From Fig. 15 and Fig. 16, it can be seen that the relationship curve $da/dN - \Delta K$ between structure and material is incomplete. The relationship curve of material depicts three stages of crack growth, including the low, medium, and high crack growth rate stages. The relationship curve of the structure is mainly to simulate the crack growth rate stage.

As shown in Fig. 16, the crack damage of the welded box girder structure of a foundry crane accumulates gradually and irreversibly with increasing cycle numbers. The fatigue crack growth is very slow from 0 (0 years) to 2,642,454 cycles (20.11 years) for the fatigue life and the crack growth size is very rapid after the crack life reaches 4,505,706 cycles (34.29 years).

5.4 Results analysis and discussion

To verify the feasibility, applicability, and accuracy of the proposed method, the analysis and discussion are carried out from three aspects: the comparison between theoretical calculation and finite element simulation results, the consideration and neglect of the dynamic response of impact load, and different calculation methods of fatigue residual life.

5.4.1 Comparison between theoretical calculation and finite element simulation results

To verify the accuracy of calculation results, the relationship between fatigue life (in unit years) and crack size in the crack propagation process of danger point 2 in Fig. 10 is transformed into the relationship between cycle number and crack size. The crack growth process defined by the relationship between cycle number and crack size is then compared with that obtained by finite element simulation, as shown in Fig. 17. Moreover, the fatigue life theoretical calculation results of danger point 2 are compared with those obtained by finite element simulation.

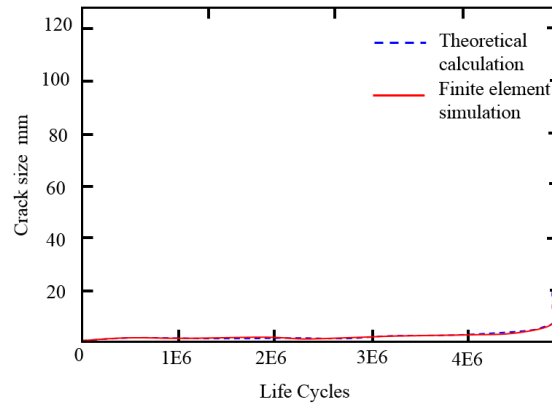


Figure 17: Comparison of theoretical calculation and finite element simulation results of the crack growth process

From Fig. 17, the fatigue crack growth simulated by finite element method is basically consistent with the theoretical results. The maximum error of crack growth size is 3.22% under the same number of stress cycles.

For fatigue life, the relative error between theoretical calculation results and simulation results is described as follows: $\delta_{life} = (37.69 - 37.37) / 37.69 = 0.849\%$. For critical crack, the relative error is $\delta_{crack} = (128.14 - 124.4) / 128.14 = 2.92\%$. Meanwhile, the fatigue crack growth simulated by the finite element method is basically consistent with the theoretical result, so the theoretical results are considered accurate.

5.4.2 Fatigue life calculations considering or not considering dynamic load effect

According to the calculation results of fatigue residual life of structures with or without load dynamic effect, the influence of load dynamic effect on the fatigue residual life of structures is discussed. The calculation results are shown in Tab. 12.

Table 12: Calculation results of fatigue life

Danger points	Considering dynamic loading effect		Without considering dynamic loading effect		Relative error of critical crack size %	Relative error of propagation life %
	Critical crack size (mm)	Crack propagation life (years)	Critical crack size (mm)	Crack propagation life (years)		
Point 1	4.11E+5	7.13E+9	4.45E+05	7.33E+9	8.27	7.43
Point 2	124.4	37.37	139.9	41.26	12.46	10.41
Point 3	150.8	74.64	160.4	81.7	6.37	9.46
Point 4	128.4	39.28	140.2	43.79	9.19	11.48
Point 5	159.2	84.19	168.3	90.05	5.72	6.96
Point 6	2.01E+5	1.75E+9	2.18E+05	1.88E+09	8.46	7.43

As given in Tab. 12, the critical crack size under dynamic loading effect is smaller than that without considering the dynamic loading effect, and the maximum error between them can be up to 12.46%. The fatigue life under dynamic loading effect is shorter, and

the maximum error is 10.41%. Thus, the load dynamic effect can accurately take into account the structural life characteristics of the foundry crane during its service. Therefore, in order to fully consider the risk of metal structure of foundry crane, the influence of load dynamic effect on fatigue life should be considered.

5.4.3 Comparative analysis of fatigue residual life based on different methods

To further verify the accuracy, feasibility, and applicability of the proposed method, it is compared with the nominal stress method in Dong et al. [Dong, Lu and Teng (2012)], hot spot stress method given in Li [Li (2014)], and Pairs model of fatigue crack growth without considering crack closure effect in Dong et al. [Dong, Xu and Xin (2018)]. The results are shown in Tab. 13.

Table 13: Fatigue residual life calculations based on different methods (years)

Danger points	Method in the paper M_1	Nominal stress method M_2	Hot spot stress method M_3	Pairs model without considering crack closure effect M_4	δ_{21}	δ_{31}	δ_{41}
Point 1	7.13E+09	8.13E+09	7.96E+09	6.99E+09	14.03	11.64	1.96
Point 2	37.37	55.37	42.54	35.37	48.17	13.83	5.35
Point 3	74.64	93.64	83.67	70.64	25.46	12.10	5.36
Point 4	39.28	60.37	44.32	36.11	53.69	12.83	8.07
Point 5	84.19	111.19	100.75	81.24	32.07	19.67	3.50
Point 6	1.75E+09	2.08E+09	1.96E+09	1.69E+09	18.86	12.00	3.43

Note : $\delta_{i1} = |M_i - M_1| / M_1 \times 100\%$, $i=2,3,4$.

From Tab. 13, compared with the method proposed in this paper, the maximum error of the results obtained by the nominal stress method, the hot spot stress method, and the Pairs model of fatigue crack growth without considering crack closure effect are 53.96%, 19.67%, and 8.07%, respectively. The reason is that the nominal stress method is simple in calculation and mature in development, but ignores the influence of local plasticity at the notch root and loading sequence. The basic assumptions do not conform to the fatigue mechanism, and the results of life assessment are unstable and low in accuracy. The hot spot stress method calculates the structural stress based on the finite element model (including welds). However, it is only suitable for the fatigue analysis of weld toes, and cannot cover the crack propagation at the weld root in the welding area. The stress range is increased by the Pairs model of fatigue crack growth considering the crack closure effect. The stress intensity factor considering the crack closure effect is lower than that without considering the crack closure effect in the process of crack growth, which hinders the propagation of cracks and effectively prolongs the fatigue life of structures. Therefore, the effect of crack closure on fatigue life should be considered from the point of actual engineering.

6 Conclusions

1) A dynamic model of the metal structures of foundry cranes in the working cycle is established by the mechanical vibration theory. The impact response coefficient of loads is analysed under diverse actions. The first principal stress-time history simulation model is established by the steel structure design criterion and multiaxial fatigue critical

interface theory. The model overcomes the deficiency of the quasi-static rule in the fatigue analysis of the metal structure of foundry cranes.

2) The fatigue life calculation formula is modified by introducing the crack closure parameters obtained by the stress ratio and effective force ratio, and the impact of the crack closure effect under residual stress on fatigue crack growth is considered.

3) The proposed method is applied to a 100/40t-28.5m eccentric rail casting crane. The feasibility and applicability of the proposed method are verified by comparing theoretical calculation with finite element simulation results in fatigue integration module Msc. Fatigue, which provides a theoretical basis for improving the anti-fatigue design of the crane.

Acknowledgement: This paper is based on the extensive investigation and testing results finished by experts and testers from Taiyuan Heavy Machinery Group Co., Ltd. The author cordially thanks experts and testers for on-site survey and real-time detection. At the same time, this paper is sponsored by the National Science-technology Support Projects for the 13th Five-year Plan (2017YFC0805703-4).

Conflicts of Interest: The authors declare that they have no conflicts of interest to report regarding the present study.

References

An, D.; Choi, J.; Kim, N. H.; Pattabhiraman, S. (2011): Fatigue life prediction based on Bayesian approach to incorporate field data into probability model. *Structural Engineering & Mechanics*, vol. 37, no. 4, pp. 427-442.

Ávila, G.; Palma, E.; Paula, R. D. (2017): Crane girder fatigue life determination using SN and LFM methods. *Engineering Failure Analysis*, vol. 79, pp. 812-819.

Brown, M. W.; Miller, K. J. (1973): A theory for fatigue failure under multiaxial stress and strain conditions. *Proceedings of the Institution of Mechanical Engineers*, vol. 187, no. 1, pp.745-755.

Cai, F. H.; Wang, X.; Zhao, F. L. (2013): A new fatigue life calculation method based on non-linear cumulative damage theory. *Applied Mechanics & Materials*, vol. 423-426, pp. 2116-2122.

Cai, F. H.; Zhao, F. L.; Gao, S. D.; Chen, L. M. (2014): Research on residual fatigue life model for lattice boom of the crane in-service. *Applied Mechanics & Materials*, vol. 875-877, pp. 1087-1094.

Chen, Y. (2018): *Fatigue Life Prediction and Reliability Analysis for the Main Beam of Polar Cranes for Nuclear Power Plants*. University of Electronic Science and Technology, Chengdu, China.

Chen, C. Y. (2002): *Fatigue and Fracture*. Huazhong University of Science and Technology Press, Wuhan, China.

Cui, C.; Zhang, Q.; Bao, Y.; Bu, Y.; Luo, Y. (2019): Fatigue life evaluation of welded joints in steel bridge considering residual stress. *Journal of Constructional Steel Research*, vol. 153, pp. 509-518.

- Dong, D. S.; Lu, C. Y.; Teng, Y. Y.** (2012): A fatigue life analysis method based on nominal stress method and MSC. FATIGUE software. *Advanced Materials Research*, vol. 468-471, pp. 663-667.
- Dong, Q.; Xu, G.; Xin, Y.** (2018): Fatigue residual life prediction of casting crane under track defect model. *Journal of Advanced Mechanical Design Systems & Manufacturing*, vol. 12, no. 4, pp. 1-16.
- Han, J.; Yang, P.; Dong, Q.** (2017): Research of overload on fatigue crack closure effect. *Journal of Wuhan University of Technology*, vol. 41, no. 5, pp. 845-858.
- Huang, N.** (2013): *Research on Fatigue Life Prediction Methods for Large-Scale Components (Ph.D. Thesis)*. Central South University, Changsha, China.
- Huang, N.; Huang, M.; Zhan, L.** (2012): Fatigue life analysis of large combination frame. *Journal of Mechanical Strength*, vol. 34, no. 2, pp. 149-153.
- Huang, N.; Huang, M.; Zhan, L.** (2012): New empirical formula of size coefficient of notched samples. *Journal of South China University of Technology*, vol. 40, no. 12, pp. 35-40.
- International Standard** (2016): ISO20332-2016 Crane-Proof of Steel Structures.
- Khaburskyi, Y.; Slobodyan, Z.; Hredil, M.; Nykyforchyn, H.** (2019): Effective method for fatigue crack arrest in structural steels based on artificial creation of crack closure effect. *International Journal of Fatigue*, vol. 127, pp. 217-221.
- Kulka, J.; Mantic, M.; Faltinova, E.; Molnar, V.; Fedorko, G.** (2018): Failure analysis of the foundry crane to increase its working parameters. *Engineering Failure Analysis*, vol. 88, pp. 25-34.
- Li, Y.** (2014): Analysis on main girder weld fatigue life of bridge crane based on hot spot stress method. *Computer Aided Engineering*, vol. 23, no. 3, pp. 44-49.
- Liu, H.** (2012): *Research on Fatigue Life of the 300t Rotary Floating Crane Structure Based on the MSC. Fatigue*. Wuhan University of Technology, Wuhan, China.
- Luo, Y.; Wu, X.; Ding, Z.; Feng, X.** (2018): Fatigue life prediction of box girder of bridge based on equivalent crack approach. *Journal of Mechanical Strength*, vol. 40, no. 1, pp. 200-204.
- Mikkola, E.; Murakami, Y.; Marquis, G.** (2014): Fatigue life assessment of welded joints by the equivalent crack length method. *Procedia Materials Science*, vol. 3, pp. 1822-1827.
- National Standards of the People's Republic of China** (2008): GB/T3811-2008 Design Rules for Cranes.
- Tao, Y. W.** (2012): *Research on Fatigue Life Prediction Technology of Tower Crane*. Xi'an University of Architecture and Technology, Xi'an, China.
- Wang, G. J.** (2009): *Fatigue Analysis Example Guidance Course*. Machinery Industry Press, Beijing, China.
- Wei, Y.** (2019): Study on the vibration of ladle cranes in accident. *China Special Equipment Safety*, no. 2, pp. 12-14.
- Wei, Z.; Dong, P.** (2010): Multiaxial fatigue life assessment of welded structures. *Engineering Fracture Mechanics*, vol. 77, no. 15, pp. 3011-3021.
- Wu, F.; Duan, Z.; Yang, X.; Qi, P.** (2019): Fatigue life analysis of quayside container

crane's based on ABAQUS and Fe-Safe. *Journal of Lanzhou Jiaotong University*, vol. 38, no. 2, pp. 80-85.

Xiang, Z. Y; Xiao, Z. M. (2015): Research on fatigue crack propagation life of casting crane girder under impact load. *Journal of Mechanical Strength*, vol. 37, no. 4, pp. 718-724.

Xu, G. N. (2018): *Mechanical Equipment Metal Structure Design*, 3rd Edition. Machinery Industry Press, Beijing, China.

Zai, J. C.; Wang, S. (1996): Variable amplitude fatigue test of box girder of bridge crane. *Journal of Taiyuan University of Science and Technology*, vol. 19, no. 2, pp. 139-144.

Zhai, J. C.; Wang, S. (1994): Fatigue test of welded box girder of bridge crane. *Hoisting and Conveing Machinery*, vol. 2, pp. 3-8.

Zhan, W. L. (2014): *Fatigue Life Prediction Based on Crack Propagation with Application in Crane Metallic Structure*. Harbin Institute of Technology, Harbin, China.